

proportional to the thickness of the target.

In summary, the transmittance of the laser through a laser-produced high- Z thin plasma is larger than that through a low- Z plasma, and the maximum transmittance through the Ni foil of $2.5\ \mu\text{m}$ thickness is larger than that through the $1.25\text{-}\mu\text{m}$ foil. The transmittance is related to energy transport through the rate of a plasma expansion. These experimental results indicate that the energy transport is due not only to superthermal electrons but also to x-ray radiation in a high- Z material. The simple theoretical calculations, based on the measurements of the electron temperature and reflectivity, qualitatively agree with the experimental conclusion.

¹G. S. Fraley, W. P. Gula, D. B. Henderson, R. L. McCrory, R. C. Malone, R. J. Mason, and R. L. Morse, in *Proceedings of the Fifth International Conference on Plasma Physics and Controlled Nuclear Fusion Research, Tokyo, 1974* (International Atomic Energy Agency, Vienna, 1975), Vol. 2, p. 543.

²R. C. Malone, R. L. McCrory, and R. L. Morse, *Phys. Rev. Lett.* **34**, 721 (1975).

³J. S. Pearlman and J. P. Anthes, *Appl. Phys. Lett.*

27, 581 (1975).

⁴B. Yaakobi, I. Pelah, and J. Hoose, *Phys. Rev. Lett.* **37**, 836 (1976).

⁵A. W. Ehler, *J. Appl. Phys.* **46**, 2464 (1975).

⁶The measurement of the angular distribution of scattered light has been reported by R. Sigel, K. Eidmann, H. C. Pant, and P. Sachsenmaier, *Phys. Rev. Lett.* **36**, 1369 (1976); B. H. Ripin, *Appl. Phys. Lett.* **30**, 134 (1977); R. A. Hass, W. C. Mead, W. L. Kruer, D. W. Phillion, H. N. Kornblum, J. D. Lindl, K. MacQuigg, V. C. Rupert, and K. G. Trisell, *Phys. Fluids* **20**, 322 (1977). Because $l < \lambda_e$ and $\lambda_e \propto \Phi_{RA}$, the heating ratio, A_e , has no strong dependence on Φ_{RA} . Then the estimate of ϕ_s does not affect the qualitative features. Assuming the total reflectivity, ϕ_s is twice as much as the value of our experiment, the ratio A_e becomes 0.5% ($4\text{-}\mu\text{m CH}_2$), 2% ($1.25\text{-}\mu\text{m Ni}$), and 3% ($2.5\text{-}\mu\text{m Ni}$), and is close to the value in the text.

⁷See Haas, Ref. 6.

⁸K. A. Brueckner, *Nucl. Fusion* **16**, 387 (1976).

⁹J. P. Freidberg, R. W. Mitchell, R. L. Morse, and L. I. Rudinski, *Phys. Rev. Lett.* **28**, 795 (1972).

¹⁰K. A. Brueckner and S. Jorna, *Rev. Mod. Phys.* **46**, 325 (1974).

¹¹Y. B. Zel'dovich and Y. P. Raizer, *Physics of Shock Waves and High-Temperature Hydrodynamic Phenomena* (Academic, New York, 1966), pp. 167, 260, and 279.

¹²M. C. Marsh and P. C. Thompson, *J. Phys. D* **8**, 383 (1975).

Studies of Doublet Plasmas in Doublet IIA

R. K. Fisher, S. J. Adcock, J. F. Baur, N. H. Brooks, J. C. DeBoo, R. L. Freeman, W. C. Guss, F. J. Helton, C. L. Hsieh, T. H. Jensen, A. F. Lietzke, J. M. Lohr, M. A. Mahdavi, K. Matsuda, C. P. Moeller, T. Ohkawa, N. Ohyabu, S. C. Prager, J. M. Rawls, T. Tamano, V. Vanek,^(a) and T. S. Wang

General Atomic Company, San Diego, California 92138

(Received 3 January 1977)

Doublet plasmas have been produced in Doublet IIA using an active field-shaping coil system. Significant increases in the electron density and energy confinement time have been observed for the doublet configuration relative to elliptic and circular plasmas in Doublet IIA.

Doublet IIA^{1,2} is a noncircular-cross-section tokamak which allows direct comparison of various plasma configurations in the same device. The ability to compare plasmas of different cross sections in the same device and within a few shots insures the same vacuum and wall conditions which are critical in tokamak operation. Detailed diagnostic measurements of the plasma properties of doublet, elliptic, and circular cross-section discharges have been performed. The measured plasma properties of the circular discharges are characteristic of those obtained in contem-

porary circular-cross-section tokamaks of similar size and toroidal field strength. The measured energy confinement time and electron density for the circular discharge are in agreement with the scaling found by Daughney³ and Murakami,⁴ respectively. A comparison of elliptic and circular plasmas produced in Doublet IIA was reported earlier.⁵ This Letter reports successful control of a doublet configuration by use of an active field-shaping coil system. Measurements on doublet discharges are presented which show a significant increase in the electron density n_e and

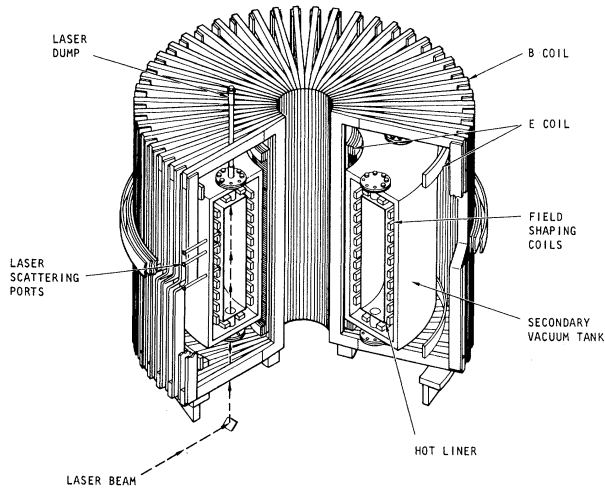


FIG. 1. Schematic view of Doublet IIA.

energy confinement time τ_E relative to values obtained in elliptic and circular discharges.

A schematic of Doublet IIA is shown in Fig. 1. The primary vacuum chamber (hot liner) has a rectangular cross section of 35 cm by 104 cm and major radius of 66 cm. The maximum plasma width is 28.5 cm determined by the tungsten limiters. The 24 field-shaping coils surrounding the plasma are used to control the plasma configuration. The air-core Ohmic heating coil (*E* coil) is driven by a capacitor-bank-transformer power supply. The toroidal field is typically 8 kG and is produced by the 48-turn *B* coil using a battery power supply. The primary and secondary vacuum chambers are separately pumped by turbomolecular pumps and the primary vacuum chamber is bakable to 300°C.

The elliptic and circular discharges were obtained by passive control of the plasma-induced image currents in the field-shaping coils using inductors and resistors.⁵ To produce a doublet configuration, it is necessary to drive additional currents in selected field-shaping coils using programmed external power supplies. The two outside midplane field-shaping coils are driven by a capacitor-bank transformer supply to push inward at the plasma midplane and form the neck of the doublet. As the plasma current-density profile peaks during Ohmic heating, a small push using a programmed silicon-controlled rectifier power supply on the top and bottom field-shaping coils is necessary to prevent a transition into a droplet configuration consisting of two separate plasmas in the top and bottom of the chamber. This approach has successfully produced doublets

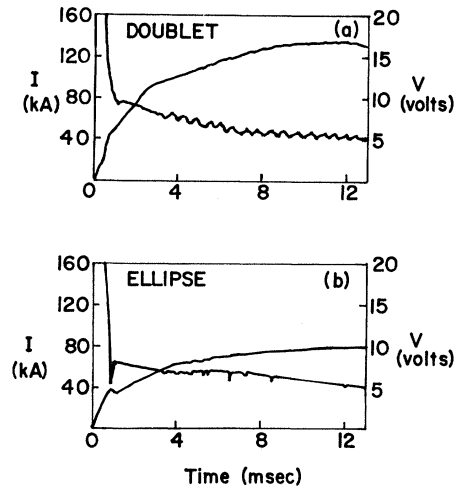


FIG. 2. Plasma current and one-turn voltage for 140-kA doublet and 75-kA elliptic discharges.

lasting the full length of the discharge, 25 to 30 msec. The plasma current and one-turn voltage for a 140-kA doublet discharge are shown in Fig. 2(a). The roughly triangular wave-form noise which appears on the voltage is due to the programming circuitry.

The magnetic flux plot for the doublet discharge is shown in Fig. 3. The details of the configuration were obtained from magnetic measurements including the voltage on one-turn loops located between the plasma and each of the field-shaping coils, and the current in each of the field-shaping coils. A free-boundary magnetohydrodynamic

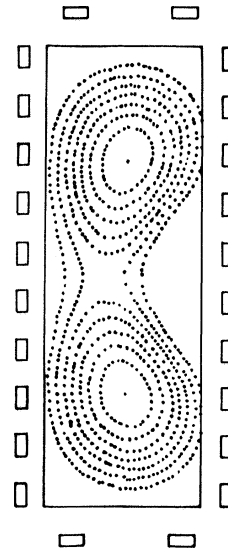


FIG. 3. Magnetic flux plot for a 140-kA doublet discharge. The positions of the 24 field-shaping coils and the limiters are also shown.

(MHD) equilibrium code⁶ is employed to calculate the magnetic configuration from the measured magnetic properties. The total plasma current and the flux values on each field-shaping coil are inputs to the code. The current-density profile and poloidal β value are adjusted to provide a fit to the 24 field-shaping coil currents and the pressure profiles measured by Thomson scattering at three different vertical locations. The measurements were taken at the time of the peak plasma current near 12 msec, and the elongation obtained is 2.9. Higher current doublets, up to 300 kA, have been obtained for several milliseconds, but hardware limitations prevented maintaining these discharges long enough to approach a steady state.

In order to compare the properties of doublet and elliptic plasmas, a 75-kA elliptic discharge, with characteristics shown in Fig. 2(b), was produced using an inductor to provide the required vertical field for radial positioning. The ellipse has a constant elongation of 1.5 from 10 to 20 msec with the peak plasma current occurring at 14 msec. Elliptic discharges with larger elongations have been produced by passively adding a quadrupole moment to the shaping field but the elongation decreases with time because of the peaking of the plasma current profile.

The plasma properties have been measured using standard tokamak diagnostic techniques including Thomson scattering, charge-exchange neutral analysis, 2-mm microwave interferometry, soft-x-ray energy analysis, visible and ultraviolet spectroscopy, and a soft-x-ray instability-detector array.

The results obtained from measurements near the time of the peak plasma current on the doublet and ellipse described above are summarized in Table I. The measurements on the elliptic discharge were taken before and after the doublet measurements to insure that the machine condition was the same. The toroidal field was 8.1 kG. The peak plasma current was 140 kA for the doublet and 75 kA for the ellipse. Radial profiles of the electron density and temperature measured by Thomson scattering for the doublet across the elliptic axis and the elliptic discharge across the midplane were very similar. The electron temperature at peak current was 350 eV for the doublet discharge and 325 eV for the elliptic discharge. This central value of the electron temperature was in agreement with that obtained by soft-x-ray energy analysis. The ion temperature was 180 eV for both the ellipse and the doublet as measured by charge exchange neutral energy analysis.

TABLE I. Plasma properties of doublet and ellipse.

	Doublet	Ellipse
B_t (kG)	8.1	8.1
I_p (kA)	140	75
T_e (eV) (center)	350	325
T_i (eV)	180	180
n_e (cm ⁻³) (center)	3.7×10^{13}	2.9×10^{13}
ϵ (elongation)	2.9	1.5
q (limiter)	5.5	2.6
q (center)	1 to 5.5	1 to 1.5
β (%) (center)	1.0	0.8
τ_E (ms) (center)	3.3 to 3.9	1.3 to 1.9
$\eta/\eta_{Sp, z=1}$	~ 4	~ 4

The central electron density measured by Thomson scattering shows a factor of about 1.3 times higher density in the doublet.

The height-to-width ratio of the outermost flux surface is 2.9 for the doublet and 1.5 for the ellipse. These values of the elongation along with the values of the safety factor were obtained from the fit to the magnetic data using the MHD code. The value obtained for the safety factor at the center of the discharges is supported by the occasional observation of $m=1$ activity on the measured soft-x-ray output. This activity was not as prominent in the doublet as in the ellipse.

The central β value, the ratio of peak plasma pressure to total magnetic pressure, was 1% in the doublet compared to 0.8% in the ellipse and 0.6% in the circular discharge with the increase resulting primarily from the increased plasma density. The central energy confinement time, τ_E , is defined by

$$\tau_E = (W_e + W_i) \times \left[j \left(E - \frac{1}{R} \frac{\partial \psi}{\partial t} \right) - \frac{\partial W_e}{\partial t} - \frac{\partial W_i}{\partial t} \right]^{-1}, \quad (1)$$

where W_e and W_i are the plasma electron and ion energy densities, j is the current density at the center, E is the measured electric field at the plasma boundary, R is the major radius, and ψ is the flux value at the plasma center. The $\partial W_i / \partial t$ term was neglected in the calculated values shown in the table, and Eq. (1) does not include a correction for radiation losses. The average energy confinement time calculated using the measured profiles is somewhat lower than the central confinement time ($\bar{\tau}_E \approx 70\% \tau_{E0}$) for each configuration. The ratio of the average confinement times for the three configurations is very

close to the ratio of the central confinement times.

The ratio of the measured plasma resistivity to the Spitzer resistivity for hydrogen is the same for both discharges. No corrections were made for trapped-particle effects. Additional information about impurity concentrations was obtained from measurements of impurity-line radiation in the visible and ultraviolet. The dominant impurity in both discharges was oxygen. Low concentrations of carbon, nitrogen, iron, chromium, and nickel were observed in both configurations.

These recent studies of shaped plasma cross sections in Doublet IIA provide a detailed comparison of doublet and elliptic discharges, while previous results⁵ provided a similar comparison of circular and elliptic discharges at a toroidal magnetic field of 7.2 kG. The circular discharge had a central electron density of $1.7 \times 10^{13} \text{ cm}^{-3}$ and a central confinement time of 1.2 msec. The elliptic discharge had properties similar to those of the elliptic discharge in Table I. The major result of the comparison was the observation of increased values of plasma density n_e and central energy confinement time τ_E in the elliptic discharge.

A further enhancement of n_e and τ_E is observed for the doublet discharges. The electron density of the doublet discharges is 1.3 times larger and the doublet τ_E is 2 to 2.5 times larger than that observed for the elliptic discharges. The $n_e \tau_E$ value of the doublet is almost 3 times the elliptic value and is 7 times the value of the circular discharge.

The cause of the improvements in n_e and τ_E is not certain. The scaling of τ_E with n_e , which is a generally accepted empirical scaling law for

circular-cross-section tokamaks, accounts for a factor of 2.2 in the improvement in the doublet τ_E relative to that observed for the circular discharge. The rest of the increase may be due to the increased volume-to-surface-area ratio consistent with $\tau_E \propto (\text{volume/surface area})^2/\chi$ and a transport coefficient χ which scales inversely with density. Thus, the transport coefficients for the three configurations all appear to be of the same magnitude. The increase in n_e is not due to an increased impurity influx. The measured densities of the oxygen, carbon, nitrogen, and iron impurities in the doublet discharges are all comparable to or smaller than those measured for the elliptic discharges.

This work was supported by the U. S. Energy Research and Development Administration, Contract No. E(04-3)-167, Project Agreement No. 38.

^(a)Present address: TRW Systems, Redondo Beach, Calif. 90277.

¹A. A. Schupp, C. C. Baker, and T. Tamano, in *Proceedings of the Fifth Symposium on Engineering Problems of Fusion Research, Princeton, New Jersey, 1973* (IEEE, New York, 1974), p. 570.

²T. Ohkawa *et al.*, in *Proceedings of the Fifth International Conference on Plasma Physics and Controlled Nuclear Fusion Research, Tokyo, Japan, 1974* (International Atomic Energy Agency, Vienna, Austria, 1975), Vol. 1, p. 291.

³C. Daughney, *Nucl. Fusion* **15**, 967 (1975).

⁴M. Murakami *et al.*, *Nucl. Fusion* **16**, 347 (1976).

⁵R. L. Freeman *et al.*, General Atomic Report No. GA-A13781, 1976 (to be published).

⁶M. S. Chu *et al.*, *Phys. Fluids* **17**, 1183 (1974).